HHS Public Access

Author manuscript

J Endocrinol. Author manuscript; available in PMC 2019 December 01.

Published in final edited form as:

J Endocrinol. 2018 December 01; 239(3): 377–388. doi:10.1530/JOE-18-0289.

Epiregulin induces leptin secretion and energy expenditure in high-fat diet-fed mice

Rumana Yasmeen[1], **Qiwen Shen**[1], **Aejin Lee**[1], **Jacob H. Leung**[1], **Devan Kowdley**[1], **David J. DiSilvestro**[1], **Lu Xu**[1,2], **Kefeng Yang**[1,3], **Andrei Maiseyeu**[4], **Naresh C. Bal**[5], **Muthu Periasamy**[5], **Paolo Fadda**[6], and **Ouliana Ziouzenkova**[1,*]

[1]Department of Human Sciences, The Ohio State University, Columbus, Ohio, 43210, USA.

[2]Department of Minimally Invasive Surgery, The First Affiliated Hospital of Soochow University, Suzhou, Jiangsu, China.

[3]Department of Nutrition, School of Medicine, Shanghai Jiao Tong University, Shanghai, China. 200025

[4]Cardiovascular Research Institute, Case Western Reserve University School of Medicine, Cleveland, OH 44106.

[5]Department of Physiology and Cell Biology, The Ohio State University, Columbus, OH 43210, USA.

[6]Nucleic Acid Shared Resource, Comprehensive Cancer Center, The Ohio State University, Columbus, Ohio 43210, USA.

Abstract

Adipokine leptin regulates neuroendocrine circuits that control energy expenditure, thermogenesis, and weight loss. However, canonic regulators of leptin secretion, such as insulin and malonyl CoA, do not support these processes. We hypothesize that epiregulin (EREG), a growth factor that is secreted from fibroblasts under thermogenic and cachexia conditions, induces leptin secretion associated with energy dissipation.

The effects of EREG on leptin secretion were studied ex vivo, in the intra-abdominal, white adipose tissue (iAb WAT) explants, as well as in vivo, in wild type mice with diet-induced obesity (DIO) and in *ob/ob* mice. These mice were pair fed a high-fat diet and treated with intraperitoneal injections of EREG.

[*]**Correspondence** Ouliana Ziouzenkova, PhD, 1787 Neil Avenue, 331A Campbell Hall; Columbus, OH 43210, ziouzenkova.1@osu.edu; Telephone: 001 614 292 5034; Fax: 001 614 292 8880.

Author contributions

R.Y. performed cell-culture studies, animal studies, generated some figures, analyzed data, and edited the manuscript. Q.S. performed cell-culture studies and assisted with animal studies. A.L. performed statistical analysis, supervised all revision experiments, and assisted with MS preparation. J.H.L. performed receptor expression studies and edited MS. D. K. performed ex-vivo studies and edited MS. D.D. performed ELISAs and edited the manuscript. X.L. assisted with animal studies. K.Y. assisted with animal studies. A.M. provided expertise for statistical analyses. N.B., M.P. provided expertise for CLAMS measurement and edited MS. P.F. provided expertise for execution of Affimetryx GeneChip, and NanoString nCounter analyses. O.Z. (PI) designed studies, analyzed and interpreted data, and wrote the manuscript.

Declaration of interest

The authors declare that there is no conflict of interest that could be perceived as prejudicing the impartiality of the research reported.

EREG increased leptin production and secretion in a dose-dependent manner in iAb fat explants via the EGFR/MAPK pathway. After 2 weeks, the plasma leptin concentration was increased by 215% in the EREG treated group compared to the control DIO group. EREG treated DIO mice had an increased metabolic rate and core temperature during the active dark cycle, and displayed cold-induced thermogenesis. EREG treatment reduced iAb fat mass, the major site of leptin secretion, but did not reduce the mass of the other fat depots. In the iAb fat, expression of genes supporting mitochondrial oxidation and thermogenesis was increased in EREG-treated mice *vs.* control DIO mice. All metabolic and gene regulation effects of EREG-treatment were abolished in leptin-deficient *ob/ob* mice.

Our data revealed a new role of EREG in induction of leptin secretion leading to the energy expenditure state. EREG could be a potential target protein to regulate hypo- and hyperleptinemia, underlying metabolic and immune diseases.

Keywords

EPR; visceral fat; obesity; thermogenesis; energy balance; EGF

Introduction

Leptin (LEP) is a critical hormone that regulates energy balance (Friedman 2016). LEP is secreted primarily by adipose tissue and has been classified as an adipokine (Friedman 2016). LEP functions are mediated by the LEP receptor (LepR) belonging to the interleukin 6 (IL-6) type family of cytokine receptors (Peelman, Zabeau, Moharana, Savvides & Tavernier 2014). LEP regulation of energy expenditure, lipolysis, basal and cold induced thermogenesis, as well as satiety, is attributed to its neuroendocrine function in the hypothalamus (Bates, Stearns, Dundon, Schubert, Tso, Wang, Banks, Lavery, Haq, Maratos-Flier *et al.* 2003). Deficiency in *Lep* is associated with severe obesity and insulin resistance in *ob/ob* mice (Friedman 2016). Similar shifts to anabolic processes occurs in human subjects with genetic *Lep* deficiency, who develop morbid obesity, and hyperphagia (Farooqi, Matarese, Lord, Keogh, Lawrence, Agwu, Sanna, Jebb, Perna, Fontana *et al.* 2002). Restoration of circulating LEP levels increases energy expenditure, decreases hyperphagia and abolishes metabolic disease in mice and humans with congenital deficiency in *Lep* (Farooqi, Matarese, Lord, Keogh, Lawrence, Agwu, Sanna, Jebb, Perna, Fontana *et al.* 2002). This fundamental and clinical research supports the notion that LEP plays a critical role in catabolic processes, culminating in energy expenditure (Friedman 2016).

Paradoxically, factors stimulating LEP secretion after feeding are attributed to a variety of anabolic factors, including glucose, insulin, glucocorticoids, mTOR, malonyl-CoA, leucine, and adenosine (Szkudelski 2007). The secretion of LEP, stimulated by these factors, does not involve regulation of *Lep* expression and is inhibited by Ca^{2+} deprivation. In response to anabolic mediators and feeding, the secretion of LEP transiently increases energy expenditure and thermogenesis (Zhang, Matheny, Tumer, Mitchell & Scarpace 2007). Moreover, the presence of LEP helps adipocytes utilize glucose for ATP production (Szkudelski 2007). However, in this scenario, LEP appears to indirectly support synthetic processes, notably, lipogenesis (Buettner, Muse, Cheng, Chen, Scherer, Pocai, Su, Cheng,

Li, Harvey-White *et al.* 2008). Combined, lipogenesis and lipolysis can increase intracellular accumulations of fatty acids, which suppress expression of *Lep* and LEP secretion in a feedback response (Szkudelski 2007). On balance, these anabolic stimuli increase LEP secretion to support an obesogenic phenotype.

In contrast, regulators of LEP secretion in catabolic settings are considerably understudied. Catabolic conditions, including cold exposure, fasting, and exercise, are all associated with a decrease in LEP secretion (Szkudelski 2007). The metabolic inducers of energy expenditure, such as intracellular cAMP and lactate, abate leptin secretion with or without insulin and glucose (Szkudelski 2007). Currently, only extracellular eicosapentaenoic fatty acid (EPA) stimulation is associated with LEP secretion that enhances mitochondrial oxidation (Perez-Matute, Marti, Martinez, Fernandez-Otero, Stanhope, Havel & Moreno-Aliaga 2005) in vitro and in vivo in association with the intra-abdominal (iAb) fat loss (Perez-Matute, Perez-Echarri, Martinez, Marti & Moreno-Aliaga 2007). It is unclear what physiological factor regulates LEP secretion in a way that supports a catabolic response.

Epiregulin (EREG) is a member of the epidermal growth factor (EGF) family ligands, including beta cellulin, heparin binding-EGF, and neuregulin (Riese & Cullum 2014). EREG binds to EGF receptor family (ERB) members EGFR (ERBB1) and ERBB4 (HER4). Under physiologic conditions, EREG is expressed in fibroblasts/preadipocytes (Toyoda, Komurasaki, Ikeda, Yoshimoto & Morimoto 1995) and tissues, including skin, lung, adipose, reproductive, and immune tissues (Riese & Cullum 2014). The current paradigm in the understanding of EREG function is based on the current belief that its sole role is as a ligand for EGFR (Riese & Cullum 2014). EREG secretion accompanies numerous physiologic processes, such as reproduction and pancreatic β-cell function. Production of EREG also occurs during inflammation and carcinogenesis (Riese & Cullum 2014), which are also accompanied by hyperleptinemia (Tessitore, Vizio, Jenkins, De Stefano, Ritossa, Argiles, Benedetto & Mussa 2000), suggesting a possible link between these pathways. Indeed, EREG forms less stable dimers with EGFR than does EGF with EGFR, which reduces EREG's carcinogenic potential (Freed, Bessman, Kiyatkin, Salazar-Cavazos, Byrne, Moore, Valley, Ferguson, Leahy, Lidke *et al.* 2017). In cancers, an association has been demonstrated between elevated EREG secretion and thermogenesis and increased energy expenditure in mouse models of cachexia (Kir, White, Kleiner, Kazak, Cohen, Baracos & Spiegelman 2014). The mechanism by which EREG could contribute to energy expenditure state remains unknown, since EREG was not able to induce direct thermogenic responses in preadipocytes (Kir, White, Kleiner, Kazak, Cohen, Baracos & Spiegelman 2014). However, thermogenic modifications in adipocytes deficient in aldehyde dehydrogenase a1 were accompanied by *Ereg* expression (Shen, Yasmeen, Marbourg, Xu, Yu, Fadda, Flechtner, Lee, Popovich & Ziouzenkova 2018). Here we test EREG efficacy in the induction of LEP secretion, in vivo and in vitro, and the relevance of this secretion for the induction of catabolic energy expenditure states.

Materials and methods

Reagents

All reagents were purchased from Sigma (St. Louis, MO) and all cell culture mediums from Life Technologies (Grand Island, NY) unless otherwise indicated. Mouse monoclonal anti-EREG antibody was purchased from Santa Cruz Biotechnology (Dallas, Texas) and secondary antibody from LI-COR Biosciences (Lincoln, NE). Mouse recombinant EREG was obtained from Sino Biological (Beijing, China). HSL (CAY10499), PI3K (Wortmannin) inhibitors were purchased from Cayman Chemical (Ann Arbor, MI). PPARα (GW6471), MAPK (U0126) inhibitors were purchased from Tocris Bioscience (Bristol, UK), and EGFR (Tyrphostin AG1478) inhibitor from Sigma-Aldrich (St. Louis, MO).

Animal studies

Animal studies were approved by the Institutional Animal Care and Use Committee of The Ohio State University (OSU).

Blinding

Animal samples were coded and data analyses were performed by personnel at the OSU Nucleic Acids Core facility who were blinded to the experimental groups.

EREG effects on WT mice fed a high-fat (HF) diet (DIO)

6-week old C57BL/6J male mice (WT) were fed a high fat diet (HF, 45% kcal from fat, D12451, Research Diet Inc., New Brunswick, NJ) for 30 days. Then, mice were randomly assigned into:

1. 1) A control group injected with 0.1mL sterile phosphate buffered saline (PBS) into both epididymal iAb fat pads (n=7), and
2. 2) EREG-treated group injected with EREG (1.5 ng/g body weight, corresponding to 20 ng per epididymal iAb fat pad) (n=7). Mice were injected with 0.1mL sterile PBS, containing 200ng EREG/mL.

Mice were individually housed and pair fed when the injections started. Mice were injected every other day for 2 weeks.

EREG effects on ob/ob mice fed a high-fat (HF) diet

6-week old *ob/ob* male mice (B6.V-Lepob/J strain containing spontaneous mutation in the gene encoding leptin congenic on C57BL/6J), purchased from the Jackson Laboratory (n=10), were fed a high fat diet (HF, 45% kcal from fat, D12451, Research Diet Inc., New Brunswick, NJ) for 30 days and then randomly assigned into two groups:

1. 1) A control group injected with 0.1mL sterile PBS into both epididymal iAb fat pads (n=5), and
2. 2) EREG-treated group injected with (EREG 2.7 ng/g body weight corresponding to 60 ng per epididymal iAb fat depot) (n=5). Mice were injected with 0.1mL sterile PBS, containing 600ng EREG/mL.

These mice were pair fed and individually housed during injections. Mice were injected every other day for 2 weeks. Metabolic measurements were performed as described below. Epididymal WAT was collected for protein, mRNA, and histology.

Comparison of lean and obese mice with dietary and genetic obesity

Three groups of mice were studied. Group 1: Four-month-old WT mice (n=8, body weight 25.9±3.8) fed regular chow (4 males and 4 females). Group 2: Three-month-old WT mice fed with HF diet (n=8, 4 males and 4 females, body weight 37.7±8.2). Mice with diet induced obesity were purchased from The Jackson Laboratory (C57BL/6J DIO) and continued on 45% HF for 3 weeks. Group 3: To compare DIO and genetically obese mice with a similar body weight we purchased 2.5-week old *ob/ob* (B6.V-Lepob/J strain containing spontaneous mutation in the gene encoding leptin congenic on C57BL/6J) mice from The Jackson Laboratory (n=8, 4 males and 4 females, body weight 43.9±6.1, P=0.13 between DIO and *ob/ob,* unpaired *t*-test). iAb perigonadal fat pads were collected as described (Yasmeen, Reichert, Deiuliis, Yang, Lynch, Meyers, Sharlach, Shin, Volz, Green *et al.* 2012) for mRNA and NanoString analysis.

Metabolic measurements

Infrared images were obtained using a camera (79R5437 FLK-TIS 9HZ Thermal Imaging Scanner: Fluke, WA). Metabolic parameters were measured by indirect calorimetry (CLAMS, Columbus Instruments, Columbus, OH) at an ambient temperature (22°C) with 12h light/dark cycles. The capacity at this facility was limited to 4 mice per study group, therefore, cold exposure and other measurements were performed with four randomly selected mice per group. Animals were fed the same HF diet and water was provided ad libitum. Mice were placed individually and allowed to acclimate to the chambers for 12h. O_2 consumption, CO_2 production, energy expenditure, and locomotor activity were measured for 24h. Then, the temperature was changed to 4°C for 6h. Based on this data, respiratory quotient, activity, exchange ratio (V_{CO2}/V_{O2}) and Δ heat values were calculated by CLAMS.

Ex-vivo Study

Epididymal iAb fat pads dissected from C57BL/6J male mice were excised into 80 mg sections for stimulation with different concentrations of EREG. Explants were stimulated with EREG in DMEM containing 1% FBS for 2h. Media was collected after 2h, lyophilized and reconstituted in 120μL deionized water for LEP detection using ELISA kit (Alpco, Salem, NH). A similar experiment was carried out where explants were stimulated with inhibitors of PPARα (GW6471, 10μM), MAPK (U0126, 10μM) and PI3K (Wortmannin, 200nM).

To analyze production of LEP, fresh epididymal iAb fat pads were collected from 12 week-old male C57BL/6J mice (n=3) and treated with or without EREG 50 ng/mL in DMEM containing 10% CS for 12h. All treated fat pads were lysed and normalized to 15 μg protein. Levels of LEP in iAb fat lysates produced and secreted into the medium were determined using ELISA kit (Crystal Chem, Elk Grove Village, IL).

Gene expression quantification by NanoString nCounter assay

NanoString's nCounter (NanoString Technologies) analysis system performs direct detection of target molecules without an amplification step. Target molecules are detected simultaneously from a single sample using color-coded molecular barcodes, giving a digital quantification of the number of target molecules. A custom panel containing *Ereg*, thermogenic genes, and PPARα–target genes was designed and used for simultaneous quantification of 37 genes, including housekeeping genes. All data were normalized to 3 housekeeping genes, *Gapdh*, *Pgk1*, and *Tubb,* and quantified in the same samples using nSolver Software. Total mRNA (100ng in 5ul) was hybridized overnight with nCounter Reporter (20μl) probes in hybridization buffer and in an excess of nCounter Capture probes (5μL) at 65°C for 16–20h. The hybridization mixture containing target/probe complexes was allowed to bind to magnetic beads containing complementary sequences on the Capture Probe. After each target found a probe pair, excess probes were washed followed by sequential binding to sequences on the Reporter Probe. Biotinylated capture probe-bound samples were immobilized and recovered on a streptavidin-coated cartridge. The abundance of specific target molecules was then quantified using the nCounter Digital Analyzer. Individual fluorescent barcodes and target molecules present in each sample were recorded with a CCD camera by performing a high-density scan (600 fields of view). Images were processed internally into a digital format and were normalized using the NanoString nSolver software analysis tool. Counts were normalized for all target RNAs in all samples based on the positive control RNA to account for differences in hybridization efficiency and post-hybridization processing, purification, and immobilization of complexes. The average was normalized by background counts (the average of the eight negative control counts) for each sample. Subsequently, a normalization of mRNA content was performed based on *Gapdh*, *Pgk1*, and *Tubb* internal reference housekeeping genes.

Semi-quantitative mRNA analysis

For analysis of EGFR and ERBB4 expressions, mRNA was isolated from epididymal iAb fat of 10 week-old male C57BL/6J mice (n=5). For other markers, mRNA was isolated from adipocyte cultures according to the manufacturer's instructions (Qiagen; Valencia, CA). cDNA was prepared from purified mRNA and analyzed using 7900HT Fast Real-Time PCR System, TaqMan fluorogenic detection system, and validated primers (Applied Biosystems; Foster City, CA). Comparative real time PCR was performed in triplicate, including no-template controls. The mRNA expression of interested genes was normalized by 18S or TATA box binding protein expression level using the comparative cycle threshold (Ct) method.

Non esterified fatty acids (NEFA) and triglyceride (TG) Assays

Plasma NEFA also (termed 'free' fatty acids) and TG were measured in plasma samples, using kits from Wako Diagnostics (Mountain View, CA).

Statistical analysis

All data are shown as mean±SD and analyzed with SPSS 25 (IBM Corp. in Armonk, NY). The number of samples is indicated in Figure legends. Group comparisons were assessed

using two-sided Student's *t*-test or analysis of variance (ANOVA) for normally distributed parameters. Mann Whitney U test or Kruskall Wallis tests were used for non-parametric values. Asterisks show $P<0.05$ that was considered to be statistically significant.

Results

EREG stimulated leptin (LEP) secretion from iAb fat ex-vivo

To investigate EREG's role in LEP secretion, we studied the effects of EREG in mouse epididymal iAb fat explants. EREG induced dose-dependent release of LEP from mouse iAb fat explants (Fig. 1A). We validated this observation using iAb fat explants from different mice. EREG stimulation increased LEP production in iAb fat (Fig. 1B), as well as its secretion into medium (Fig. 1C). EREG mediated its signaling primarily via EGF receptor (EGFR), which leads to MAPK activation (Roskoski 2014). *Egfr* was abundantly expressed in iAb fat, whereas *Erbb4* expression was low (Fig. 1D). EREG-dependent LEP secretion was moderately decreased with EGFR inhibitor, tyrphostin, and abolished with the MAPK inhibitor, U0126 (Fig. 1E). PI3K activation was also reported downstream of EREG activation of EGFR (Roskoski 2014); however, inhibition of PI3K did not influence LEP secretion by EREG (Fig. 1F). Given that LEP secretion could depend on intracellular lipid status, *e.g.* EPA hydrolysis, we inhibited hormone sensitive lipase (HSL) and PPARα transcriptional response. However, inhibitors of HSL and PPARα did not disrupt EREG-mediated activation of LEP secretion (Fig. 1F). We concluded that EREG is a candidate inducer of LEP secretion via EGFR/MAPK signaling cascade.

EREG stimulated LEP secretion in mice with diet-induced obesity (DIO)

We examined the effect of EREG on LEP secretion in wild-type (WT) mice challenged with a high-fat diet (DIO mice). We selected a short treatment time to minimize inflammatory and injury responses related to injections. DIO mice were treated six times with EREG (1.5 ng/g body weight) over a period of 2 weeks. EREG injections into iAb fat had no significant effect on *Lep* expression in both EREG-treated and control DIO groups (Fig. 2A). However, the plasma levels of secreted LEP were 215% higher in EREG-treated *vs.* non-treated mice (Fig. 2B). EREG treatments also increased the levels of non-esterified fatty acids (NEFA) in plasma (587% in EREG-treated compared to control DIO mice) (Fig. 2C). In contrast, plasma triglyceride (TG) levels were reduced by 47.6% in EREG-treated vs. control DIO mice (Fig. 2D).

EREG increased energy expenditure and iAb fat loss in DIO mice

Next, we measured the association of LEP secretion with a catabolic phenotype in EREG treated mice. Metabolic rate was calculated based on rate of oxygen consumption measured in the acclimated, individually housed mice for 24 hours at an ambient temperature (RT) and after 6 hours cold-exposure in metabolic cages. The basal metabolic rate was identical during resting periods in both groups (Fig. 3A, left). However, during the active dark period, metabolic rate was higher in EREG-treated compared to non-treated DIO mice at RT (Fig. 3A, left) and after cold exposure (Fig. 3A, right). The EREG-treated DIO mice reached a maximal metabolic rate plateau in a significantly shorter period of time compared to the control group during the cold exposure (Fig. 3B). The locomotor activity during light and

dark period at RT, as well as during cold exposure, was similar between DIO groups (Fig. 3C). Respiratory exchange ratio (RER) was not statistically different between groups; however, EREG mice maintained RER values above 0.8, indicating glucose was their main source for energy (Fig. 3D). The body temperature in DIO mice was assessed based on infrared scanning. The intensities were quantified as the differences in the intensities following cold exposure and basal values obtained at RT (Fig. 3E). EREG treatment significantly increased abdominal core body temperature compared to control DIO mice in agreement with the increased metabolic rate in these mice (Fig. 3A). The increase in abdominal core body temperature occurred within areas containing epididymal iAb fat (Fig. 3E, arrows). These areas were highlighted after subtraction of temperatures before and after cold exposure (Fig. 3E, right panels). These data support increased energy expenditure in response to EREG treatment in DIO mice.

EREG increased iAb fat loss in mice

In our experiment, EREG treatment has a modest effect (range 0–5% compared to the initial weight) on weight regulation (Fig. 4A) in DIO mice with food intake controlled by pair feeding (Fig. 4B). The comparison of weight changes before and after EREG treatment indicated minor, but significant differences in DIO mice treated with EREG (Fig. 4A). The weight changes in the control group fluctuated and were not significant. EREG treatments did not influence liver weight (Fig. 4C). Both EREG and control mice groups had similar weight of brown fat (Fig. 4D) and subcutaneous WAT (Fig. 4E). The difference in weight resulted from changes in the epididymal iAb WAT. EREG-treated mice had 32% less iAb fat than non-treated mice (Fig. 4F). Given that the increase in thermogenesis was also associated with the iAb fat location (Fig. 3E), we analyzed the expression of genes regulating thermogenesis and mitochondrial oxidative phosphorylation in this fat depot.

EREG induced genes associated with oxidative phosphorylation and thermogenesis

Gene expression was quantified simultaneously for all measured genes and housekeeping genes using NanoString assay. An analysis of gene expression in iAb fat showed similar expression of *Pparg* (Fig. 5A) and *Ppara* (Fig. 5B) in EREG-treated and control DIO mice. However, we found an increased expression of the PPARα target genes, *Mcad,* and Cpt2 (Fig. 5B), and genes supporting mitochondrial oxidation, e.g. *CoxIV* (Fig. 5C), in the iAb fat of EREG-treated *vs*. non-treated DIO mice. EREG treatment induced increased expression of *Pgc1a*, *Cidea* genes (197% and 275%, respectively, compared to 100% expression seen in iAb fat in the control DIO group, Fig. 5D). Similarly there was a 179% increase in *Rip140* (Fig. 5E) and a 187% increase in *Dio2* (Fig. 5F) expression in the iAb fat was associated with EREG-treatment vs non-treated DIO. These genes are established regulators of oxidative phosphorylation and thermogenesis (Kir, White, Kleiner, Kazak, Cohen, Baracos & Spiegelman 2014). These differences in thermogenesis were not associated with the increased levels of brown adipocytes, since the expression of brown adipose tissue (BAT) marker *Prdm16* was similar between groups (Fig. 5F). Although *Ucp1* expression was increased 2-fold in EREG-treated *vs.* control group, it was not significant due to the substantial variation within the treated group (Fig. 5F). In other studies in 3T3-L1 adipocytes (Kir, White, Kleiner, Kazak, Cohen, Baracos & Spiegelman 2014), high concentrations of EREG induced robust *Ucp1* expression. We also assessed a possible

contribution of inflammation to energy expenditure mediated by EREG/LEP. The expression of pro-inflammatory genes, *Tnfa* and *Mcp1*, were suppressed in EREG *vs.* control group (Fig. 5G). The expression of *CD137*, activated in regulatory lymphocytes, was similar in both groups. Therefore, EREG treatment increased mitochondrial and thermogenic gene expression without triggering inflammation. We also examined the effect of dietary and genetic obesity in *Ereg* expression in the iAb fat (Fig. 5H). *Ereg* expression in the iAb fat saw a similar increase in both DIO and *ob/ob* mice compared to the lean mice group. Moreover, *Ereg* expression within all groups was not sex-dependent. Next, we tested whether EREG can induce similar energy expenditure in *ob/ob* in the absence of LEP, as in DIO mice.

EREG regulated energy expenditure and iAb gene expression in a Lep-dependent manner

We treated *ob/ob* mice fed the same high-fat diet with recombinant EREG (2.7 ng/g body weight) for two weeks. Due to a high amount of iAb fat in the intraperitoneal cavity of the *ob/ob* mice, we increased the dose of EREG to ensure adequate exposure to EREG. Treatment with EREG in *ob/ob* mice did not prevent weight gain in these mice (Fig. 6A). We pair fed *ob/ob* mice from both groups to achieve identical food intake (Fig. 6A, insert). EREG-treatment did not alter weight in any investigated tissue, including the liver (Fig. 6B), BAT (Fig. 6C), subcutaneous and iAb WAT depots (Fig. 6D).

The EREG-treatment did not influence metabolic changes during the active dark cycle. However, *ob/ob* mice treated with EREG had significantly lower RER during the light cycle (Fig. 6E) compared to the control *ob/ob* mice. The cold exposure decreased RER levels in the control *ob/ob* mice that reached levels observed in the EREG-treated group (Fig. 6E). These RER values suggest equal utilization of glucose and lipid substrates in both groups after cold exposure. *Ob/ob* mice treated with EREG also exhibited higher locomotor activity after transition from ambient temperature to cold (Fig. 6F), whereas the activity in the control *ob/ob* mice was similar at ambient and cold temperatures. Notably, the metabolic rate did not undergo circadian changes (Fig. 6G) and remained identical between EREG-treated and control *ob/ob* groups before and during cold exposure (Fig. 6H). In the iAb fat of *ob/ob* mice, the expression levels of all PPARα target genes and mitochondrial genes involved in thermogenesis and oxidative phosphorylation were similar between control and EREG treated groups (Fig. 6I). Given that all effects of EREG related to regulation of energy expenditure in DIO mice were abolished in *ob/ob* mice, we concluded that EREG mediates its energy expenditure effects via systemic secretion of LEP.

Discussion

LEP is a pivotal adipokine which regulates energy expenditure under anabolic and catabolic conditions in order to maintain energy balance (Friedman 2016). The well-established regulators of LEP secretion, such as insulin, regulate anabolic processes underlying growth and development, as well as pathogenesis of obesity and diabetes in adults (Szkudelski 2007). Our studies revealed that EREG is an inducer of LEP production and secretion, which maintained energy expenditure state in obese DIO mice. In these mice, EREG-regulated central energy expenditure responses resulted in the circadian increase in metabolic rate and

rise in body temperature after cold exposure. EREG function in the regulation of energy expenditure was dependent on LEP and abolished in *ob/ob* mice. Similar to anabolic inducers of LEP secretion, including insulin (Szkudelski 2007), EREG increased LEP secretion without up-regulation of *Lep* expression in WAT. The studies with pharmacological inhibitors suggest that EREG utilized canonic EGFR receptor MAPK signaling pathway (Yamanaka, Hayashi, Komurasaki, Morimoto, Ogihara & Sobue 2001) to increase LEP secretion. However, further studies are necessary to understand the mechanisms eliciting secretion of LEP.

A distinctive aspect of EREG-mediated LEP secretion is an occurrence of tissue-specific effects in iAb fat. We injected EREG in iAb fat; however, EREG was expected to reach systemic circulation. We observed that increased core temperature after the cold exposure reduced accumulation of WAT in iAb depot in EREG treated DIO mice. These responses were in agreement with the increased expression of genes supporting mitochondrial oxidation and thermogenesis in the iAb fat in EREG-treated mice. This tissue-specific sensitivity of iAb WAT to EREG was also dependent on LEP and abolished in *ob/ob* mice. The specific effects related to core body temperature (Kaiyala, Ogimoto, Nelson, Muta & Morton 2016) and iAb tissue have been previously reported for LEP. The circadian increase in core body temperature during cold exposure was also observed in *ob/ob* mice treated with LEP (Kaiyala, Ogimoto, Nelson, Muta & Morton 2016). This effect was not dependent on the sympathetic activation of uncoupling protein 1 (UCP1) thermogenesis in the BAT depots, because the denervation of BAT does not prevent weight loss induced by LEP (Cote, Sakarya, Green, Morgan, Carter, Tumer & Scarpace 2018). Although the mechanism for these LEP effects has not been fully elucidated, two hypotheses, based on the humoral (Ukropec, Anunciado, Ravussin & Kozak 2006) and neuroregulatory role (Niijima 1998) of LEP, have been proposed for the control of thermogenesis and lipolysis in a fat depot-specific manner (Niijima 1998). The neuroregulatory hypothesis proposes different innervation of WAT depots (reviewed in (Bartness, Liu, Shrestha & Ryu 2014)). In response to LEP, neurons stimulate lipolysis in an adipose-depot specific manner. EREG treatment in our studies also increased NEFA levels, but decreased TG levels in the circulation, which was accompanied by reduction in the iAb fat. These findings suggest that EREG-induced LEP release facilitated lipolysis in this fat depot. Other studies deciphering the specific role of LEP in thermogenesis have proposed humoral regulation via T3 dependent pathways (Ukropec, Anunciado, Ravussin & Kozak 2006), including upregulation of *Dio2*. This is an alternative pathway for induction of thermogenesis, which does not require UCP1 (Ukropec, Anunciado, Ravussin & Kozak 2006). In this study, we also observed humoral regulation of thermogenesis that was related to T3 metabolism. Mice treated with EREG expressed higher levels of *Dio2* and *Cidea* in the iAb fat compared to the control DIO mice. Moreover, these thermogenic changes proceed without upregulation of *Prdm16*. Similar gene regulation, involved in thermogenic response and mitochondrial oxidation, was found in rats treated with *Lep*-expressing adenovirus (Zhou, Wang, Higa, Newgard & Unger 1999). Cao and co-workers proposed that this gene regulation can effectively reduce iAb fat depots (Yang, Sui, Zhang, Dong, Lim, Seki, Guo, Fischer, Lu, Zhang *et al.* 2017). Both studies are in agreement with the proposed function of EREG as an upstream regulator of LEP secretion. Thus, EREG/LEP axes appear to utilize both neuroregulatory and humoral pathways for the

regulation of iAb fat. Compared to other adipose depots, iAb obesity poses the highest risk for development of cardiovascular disease, cancer, and diabetes that, together, contribute to the overall increase in mortality in people accumulating iAb WAT (Zhang, Rexrode, van Dam, Li & Hu 2008). EREG-dependent activation of LEP secretion provides an important insight into the etiology of iAb fat formation and mechanisms of its reduction.

Our data provide an important cue to the understanding of the physiological and pathophysiological role of EREG. EREG was cloned from the 3T3-L1 cell line derived from WAT (Toyoda, Komurasaki, Ikeda, Yoshimoto & Morimoto 1995) and, subsequently, from a variety of other tissues, including various cancers (Toyoda, Komurasaki, Uchida & Morimoto 1997). EREG induces prolonged activation of EGFR receptor dimers, which promotes breast cancer cell differentiation rather than proliferation (Freed, Bessman, Kiyatkin, Salazar-Cavazos, Byrne, Moore, Valley, Ferguson, Leahy, Lidke *et al.* 2017). Although this mechanism limits EREG's carcinogenic potential, EREG production in cancer cells or in the iAb fat can potentially influence central and local concentrations of LEP. In breast cancer, the levels of LEP are elevated (Tessitore, Vizio, Jenkins, De Stefano, Ritossa, Argiles, Benedetto & Mussa 2000), but show an opposite association with cachexia in males (positive correlation) and females (negative correlation). Our work was limited to studying EREG's role in male metabolism, although *Ereg* is expressed in iAb fat of males and females. However, the energy dissipation state produced by EREG-dependent-secretion of LEP may shed light on the understanding of cancer energetics, at least in males.

EREG and EGF signaling via EGFR control numerous physiologic processes in cellular growth, proliferation, and tissue regeneration. We found that EREG can regulate RER and locomotor activity during the inactive light cycle in *ob/ob*. These data could be interpreted as a compensatory effect, increasing thermic responses in skeletal muscle. In this setting, EREG acted independently of LEP. Recent studies ascribed many functions in reproduction (Kim, Lee, Threadgill & Lee 2011; Park, Su, Ariga, Law, Jin & Conti 2004; Shiraishi & Matsuyama 2012), β cell growth and insulin secretion (Kuntz, Broca, Komurasaki, Kaltenbacher, Gross, Pinget & Damge 2005), and immunity (Sugiyama, Nakabayashi, Baba, Sasazuki & Shirasawa 2005) specifically to EREG. Notably, LEP effects regulate these pathways (Friedman 2016; Han, Yamamoto, Munesue, Motoyoshi, Saito, Win, Watanabe, Tsuneyama & Yamamoto 2013; Hu, Han, Cao, Mao-Ying, Mi & Wang 2018; Mattioli, Straface, Matarrese, Quaranta, Giordani, Malorni & Viora 2008). Future studies will decipher a dependence of EREG effects on LEP secretion and identify possible molecular crosstalk between these pathways in different physiological and pathologic settings (Wauman, Zabeau & Tavernier 2017). In our studies, the majority of EREG responses were dependent on LEP. A novel function of EREG in the regulation of LEP secretion could be used to balance hypo- and hyperleptinemia states and regulate energy utilization.

Acknowledgments

Funding

This work was funded by the Novo Nordisk Pharmaceuticals (10040042) (O.Z., Q.S., A.L., R.Y., X.L., KY, D.D.S). The project was supported by NIH grants R21OD017244 (O.Z., Q.S., R.Y., X.L., KY, D.D.S), HL130516 (A.M) the National Center for Research Resources UL1RR025755 and NCI CCSGP30CA16058 and CCSG: P30CA016058 (OSUCCC) (P.F.), the NIH Roadmap for Medical Research, Technical and Commercialization Office at OSU, and

SEED grant and Brain Injury Program at OSU (O.Z., A.L., J.H.L., D.K.). The content is solely the responsibility of the authors and does not necessarily represent the official views of the National Center for Research Resources or the National Institutes of Health.

Abbreviations:

BAT	brown adipose tissue
DIO	diet-induced obese wild type mice
EGF	epidermal growth factor
EGFR	EGF receptor
EREG	epiregulin
HSL	hormone sensitive lipase
iAb	intra-abdominal
Lep	leptin
LepR	leptin receptor
MAPK	mitogen activated protein kinase
NEFA	non-esterified fatty acids
PPAR	Peroxisome proliferator-activated receptor
RER	respiratory exchange ratio
T1D	type 1 diabetes
TG	triglyceride
UCP1	uncoupling protein 1
WAT	white adipose tissue

References

Bartness TJ, Liu Y, Shrestha YB, & Ryu V 2014 Neural innervation of white adipose tissue and the control of lipolysis. Frontiers in neuroendocrinology 35 473–493. (10.1016/j.yfrne.2014.04.001) [PubMed: 24736043]

Bates SH, Stearns WH, Dundon TA, Schubert M, Tso AW, Wang Y, Banks AS, Lavery HJ, Haq AK, Maratos-Flier E, et al. 2003 STAT3 signalling is required for leptin regulation of energy balance but not reproduction. Nature 421 856–859. (10.1038/nature01388) [PubMed: 12594516]

Buettner C, Muse ED, Cheng A, Chen L, Scherer T, Pocai A, Su K, Cheng B, Li X, Harvey-White J, et al. 2008 Leptin controls adipose tissue lipogenesis via central, STAT3-independent mechanisms. Nature medicine 14 667–675. (10.1038/nm1775)

Cote I, Sakarya Y, Green SM, Morgan D, Carter CS, Tumer N, & Scarpace PJ 2018 iBAT sympathetic innervation is not required for body weight loss induced by central leptin delivery. American journal of physiology Endocrinology and metabolism 314 E224–E231. (10.1152/ajpendo.00219.2017) [PubMed: 29089334]

Farooqi IS, Matarese G, Lord GM, Keogh JM, Lawrence E, Agwu C, Sanna V, Jebb SA, Perna F, Fontana S, et al. 2002 Beneficial effects of leptin on obesity, T cell hyporesponsiveness, and neuroendocrine/metabolic dysfunction of human congenital leptin deficiency. J Clin Invest 110 1093–1103. (10.1172/JCI15693) [PubMed: 12393845]

Freed DM, Bessman NJ, Kiyatkin A, Salazar-Cavazos E, Byrne PO, Moore JO, Valley CC, Ferguson KM, Leahy DJ, Lidke DS, et al. 2017 EGFR Ligands Differentially Stabilize Receptor Dimers to Specify Signaling Kinetics. Cell 171 683–695 e618. (10.1016/j.cell.2017.09.017) [PubMed: 28988771]

Friedman J 2016 The long road to leptin. J Clin Invest 126 4727–4734. (10.1172/JCI91578) [PubMed: 27906690]

Han D, Yamamoto Y, Munesue S, Motoyoshi S, Saito H, Win MT, Watanabe T, Tsuneyama K, & Yamamoto H 2013 Induction of receptor for advanced glycation end products by insufficient leptin action triggers pancreatic beta-cell failure in type 2 diabetes. Genes to cells : devoted to molecular & cellular mechanisms 18 302–314. (10.1111/gtc.12036) [PubMed: 23410183]

Hu ZJ, Han W, Cao CQ, Mao-Ying QL, Mi WL, & Wang YQ 2018 Peripheral Leptin Signaling Mediates Formalin-Induced Nociception. Neuroscience bulletin 34 321–329. (10.1007/s12264-017-0194-2) [PubMed: 29204732]

Kaiyala KJ, Ogimoto K, Nelson JT, Muta K, & Morton GJ 2016 Physiological role for leptin in the control of thermal conductance. Molecular metabolism 5 892–902. (10.1016/j.molmet.2016.07.005) [PubMed: 27689002]

Kim K, Lee H, Threadgill DW, & Lee D 2011 Epiregulin-dependent amphiregulin expression and ERBB2 signaling are involved in luteinizing hormone-induced paracrine signaling pathways in mouse ovary. Biochemical and biophysical research communications 405 319–324. (10.1016/j.bbrc.2011.01.039) [PubMed: 21237132]

Kir S, White JP, Kleiner S, Kazak L, Cohen P, Baracos VE, & Spiegelman BM 2014 Tumour-derived PTH-related protein triggers adipose tissue browning and cancer cachexia. Nature 513 100–104. (10.1038/nature13528) [PubMed: 25043053]

Kuntz E, Broca C, Komurasaki T, Kaltenbacher MC, Gross R, Pinget M, & Damge C 2005 Effect of epiregulin on pancreatic beta cell growth and insulin secretion. Growth factors 23 285–293. (10.1080/08977190500233367) [PubMed: 16338791]

Mattioli B, Straface E, Matarrese P, Quaranta MG, Giordani L, Malorni W, & Viora M 2008 Leptin as an immunological adjuvant: enhanced migratory and CD8+ T cell stimulatory capacity of human dendritic cells exposed to leptin. FASEB journal : official publication of the Federation of American Societies for Experimental Biology 22 2012-2022. (10.1096/fj.07-098095) [PubMed: 18218920]

Niijima A 1998 Afferent signals from leptin sensors in the white adipose tissue of the epididymis, and their reflex effect in the rat. Journal of the autonomic nervous system 73 19–25. [PubMed: 9808367]

Park JY, Su YQ, Ariga M, Law E, Jin SL, & Conti M 2004 EGF-like growth factors as mediators of LH action in the ovulatory follicle. Science 303 682–684. (10.1126/science.1092463) [PubMed: 14726596]

Peelman F, Zabeau L, Moharana K, Savvides SN, & Tavernier J 2014 20 years of leptin: insights into signaling assemblies of the leptin receptor. J Endocrinol 223 T9–23. (10.1530/JOE-14-0264) [PubMed: 25063754]

Perez-Matute P, Marti A, Martinez JA, Fernandez-Otero MP, Stanhope KL, Havel PJ, & Moreno-Aliaga MJ 2005 Eicosapentaenoic fatty acid increases leptin secretion from primary cultured rat adipocytes: role of glucose metabolism. American journal of physiology Regulatory, integrative and comparative physiology 288 R1682–1688. (10.1152/ajpregu.00727.2004)

Perez-Matute P, Perez-Echarri N, Martinez JA, Marti A, & Moreno-Aliaga MJ 2007 Eicosapentaenoic acid actions on adiposity and insulin resistance in control and high-fat-fed rats: role of apoptosis, adiponectin and tumour necrosis factor-alpha. The British journal of nutrition 97 389–398. (10.1017/S0007114507207627) [PubMed: 17298710]

Riese DJ, 2nd, & Cullum RL 2014 Epiregulin: roles in normal physiology and cancer. Semin Cell Dev Biol 28 49–56. (10.1016/j.semcdb.2014.03.005) [PubMed: 24631357]

Roskoski R, Jr. 2014 The ErbB/HER family of protein-tyrosine kinases and cancer. Pharmacological research 79 34–74. (10.1016/j.phrs.2013.11.002) [PubMed: 24269963]

Shen Q, Yasmeen R, Marbourg J, Xu L, Yu L, Fadda P, Flechtner A, Lee LJ, Popovich PG, & Ziouzenkova O 2018 Induction of innervation by encapsulated adipocytes with engineered vitamin A metabolism. Translational research : the journal of laboratory and clinical medicine 192 1–14. (10.1016/j.trsl.2017.10.005) [PubMed: 29144959]

Shiraishi K, & Matsuyama H 2012 Local expression of epidermal growth factor-like growth factors in human testis and its role in spermatogenesis. Journal of andrology 33 66–73. (10.2164/jandrol.110.011981) [PubMed: 21273504]

Sugiyama S, Nakabayashi K, Baba I, Sasazuki T, & Shirasawa S 2005 Role of epiregulin in peptidoglycan-induced proinflammatory cytokine production by antigen presenting cells. Biochemical and biophysical research communications 337 271–274. (10.1016/j.bbrc.2005.09.050) [PubMed: 16182244]

Szkudelski T 2007 Intracellular mediators in regulation of leptin secretion from adipocytes. Physiological research 56 503–512. [PubMed: 17184148]

Tessitore L, Vizio B, Jenkins O, De Stefano I, Ritossa C, Argiles JM, Benedetto C, & Mussa A 2000 Leptin expression in colorectal and breast cancer patients. International journal of molecular medicine 5 421–426. [PubMed: 10719061]

Toyoda H, Komurasaki T, Ikeda Y, Yoshimoto M, & Morimoto S 1995 Molecular cloning of mouse epiregulin, a novel epidermal growth factor-related protein, expressed in the early stage of development. FEBS letters 377 403–407. (10.1016/0014-5793(95)01403-9) [PubMed: 8549764]

Toyoda H, Komurasaki T, Uchida D, & Morimoto S 1997 Distribution of mRNA for human epiregulin, a differentially expressed member of the epidermal growth factor family. The Biochemical journal 326 **(** Pt 1**)** 69–75. [PubMed: 9337852] **()**

Ukropec J, Anunciado RV, Ravussin Y, & Kozak LP 2006 Leptin is required for uncoupling protein-1-independent thermogenesis during cold stress. Endocrinology 147 2468–2480. (10.1210/en.2005-1216) [PubMed: 16469807]

Wauman J, Zabeau L, & Tavernier J 2017 The Leptin Receptor Complex: Heavier Than Expected? Frontiers in endocrinology 8 30 (10.3389/fendo.2017.00030) [PubMed: 28270795]

Yamanaka Y, Hayashi K, Komurasaki T, Morimoto S, Ogihara T, & Sobue K 2001 EGF family ligand-dependent phenotypic modulation of smooth muscle cells through EGF receptor. Biochemical and biophysical research communications 281 373–377. (10.1006/bbrc.2001.4385) [PubMed: 11181057]

Yang X, Sui W, Zhang M, Dong M, Lim S, Seki T, Guo Z, Fischer C, Lu H, Zhang C, et al. 2017 Switching harmful visceral fat to beneficial energy combustion improves metabolic dysfunctions. JCI insight 2 e89044 (10.1172/jci.insight.89044) [PubMed: 28239649]

Yasmeen R, Reichert B, Deiuliis J, Yang F, Lynch A, Meyers J, Sharlach M, Shin S, Volz KS, Green KB, et al. 2012 Autocrine Function of Aldehyde Dehydrogenase 1 as a Determinant of Diet- and Sex-Specific Differences in Visceral Adiposity. Diabetes. (10.2337/db11-1779)

Zhang C, Rexrode KM, van Dam RM, Li TY, & Hu FB 2008 Abdominal obesity and the risk of all-cause, cardiovascular, and cancer mortality: sixteen years of follow-up in US women. Circulation 117 1658–1667. (https://doi.org/CIRCULATIONAHA.107.739714 [pii] 10.1161/CIRCULATIONAHA.107.739714) [PubMed: 18362231]

Zhang J, Matheny MK, Tumer N, Mitchell MK, & Scarpace PJ 2007 Leptin antagonist reveals that the normalization of caloric intake and the thermic effect of food after high-fat feeding are leptin dependent. *American journal of physiology* Regulatory, integrative and comparative physiology 292 R868–874. (10.1152/ajpregu.00213.2006)

Zhou YT, Wang ZW, Higa M, Newgard CB, & Unger RH 1999 Reversing adipocyte differentiation: implications for treatment of obesity. Proc Natl Acad Sci U S A 96 2391–2395. [PubMed: 10051652]

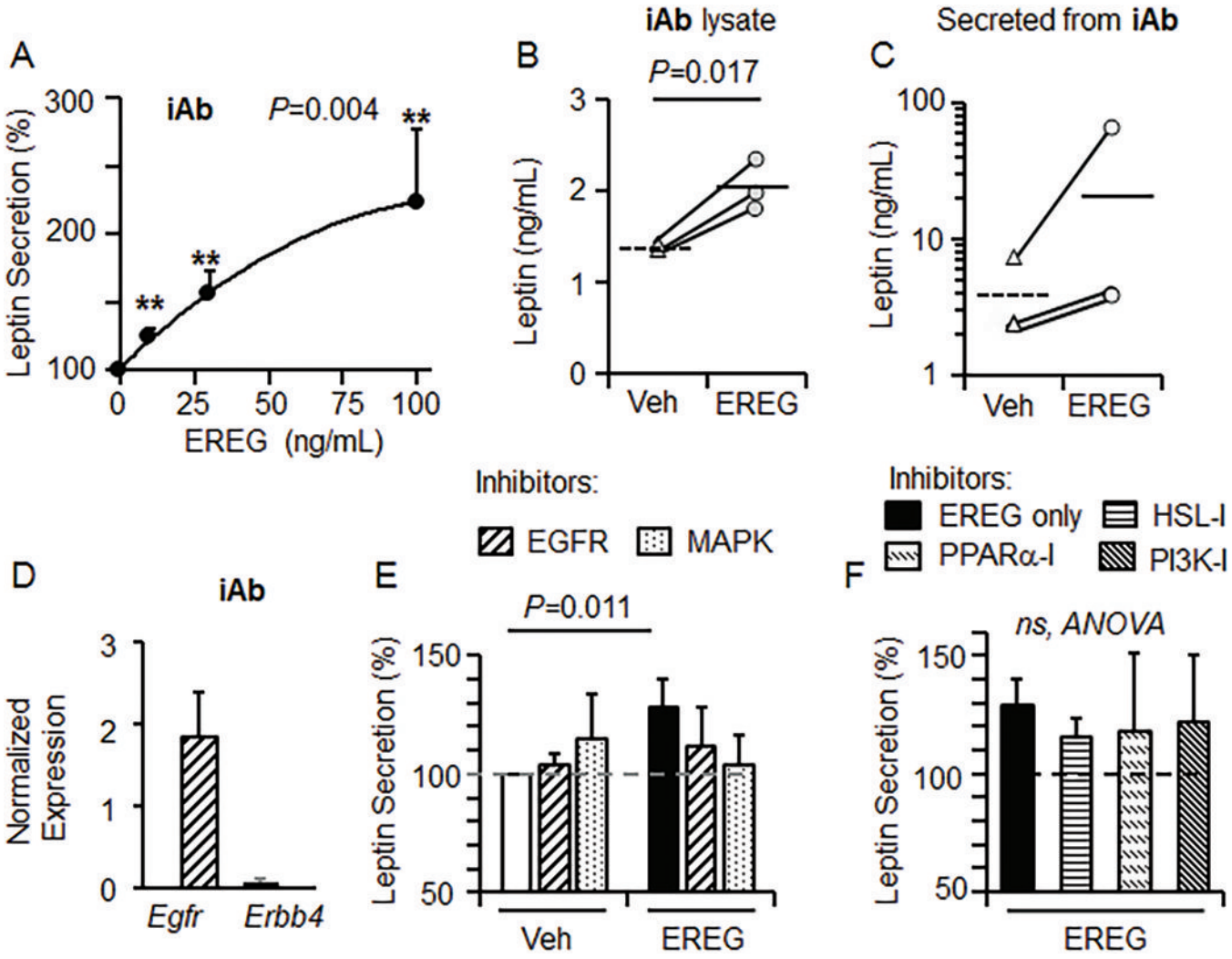

Figure 1.

EREG/EGFR/MAPK axes induced leptin (LEP) secretion from adipose tissues ex vivo. Five iAb epididymal fat explants were excised from WT mice and stimulated. After 2h of stimulation LEP levels were measured in the media by ELISA. This experiment was repeated in three different WT mice. (A) Concentration-dependent secretion of LEP in the media from iAb fat explants stimulated with different concentrations of EREG. Data (mean ±SD, n=5) are shown as percent to control (Veh, 100 %). Kruskal Wallis test. (B, C) LEP concentrations in the iAb fat lysates (B) and media (C) released from iAb fat before (triangles) and after (circles) stimulation with EREG (black bar, 50 ng/ml). Dashed and solid lines show mean value (n=3 mice) before and after stimulation. (D) Expression levels of *Egfr* and *Erbb4* in epididymal iAb fat of lean WT mice (mean±SD, n=5) were measured by RT-PCR and normalized by TBP. (E) LEP concentrations in the iAb fat stimulated with EREG (black bar, 50 ng/ml) in the presence and absence of inhibitors of EGFR (10 μM) and MAPK (10 μM). Data (mean±SD, n=5) are shown as percent to control (Veh, white bar, 100%, dashed line). Between subject ANOVA with post-hoc Fisher LSD group comparison (α=0.05). (F) LEP in the media released following stimulation of mouse explants with and

without EREG (50 ng/mL) in the presence and absence of inhibitors of HSL (10 μM), PPARα (10 μM), and PI3K (100 nM). Data (mean±SD, n=5) are shown as percent of control (Veh, 100%, dashed line). Between subject ANOVA. *ns*: not significant.

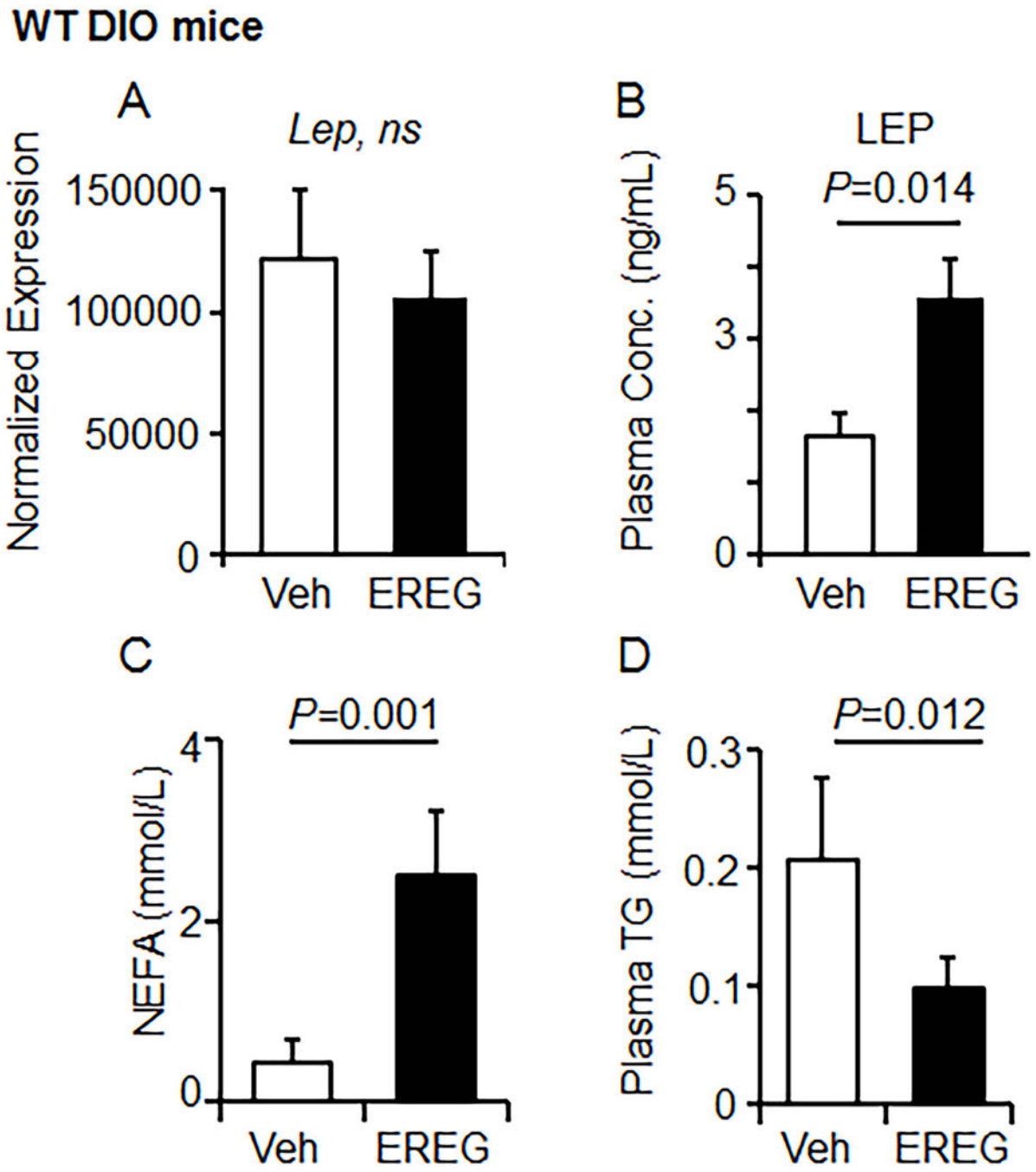

Figure 2.

EREG stimulates leptin secretion and lipolysis in mice with diet-induced obesity (DIO). (A) DIO WT male mice (n=7/ group) were injected with 100μL PBS (Veh) with and without EREG (1.5ng/g body weight or 20ng/per iAb depot) into both epididymal iAb fat pads every other day for 2 weeks. Total mRNA was isolated from one whole iAb fad pad. Expression of *Lep* was measured using NanoString assay. Normalized data represent mean±SD, n=5; Mann-Whitney U test. (B) Expression of LEP protein levels were measured in plasma in the same mice group by ELISA. Data (mean±SD, n=5/group). Independent Student's *t*-test. (C)

Non-esterified fatty acids (NEFA) and (D) TG concentrations in plasma are shown as mean ± SD, n=5. Independent Student's *t*-test.

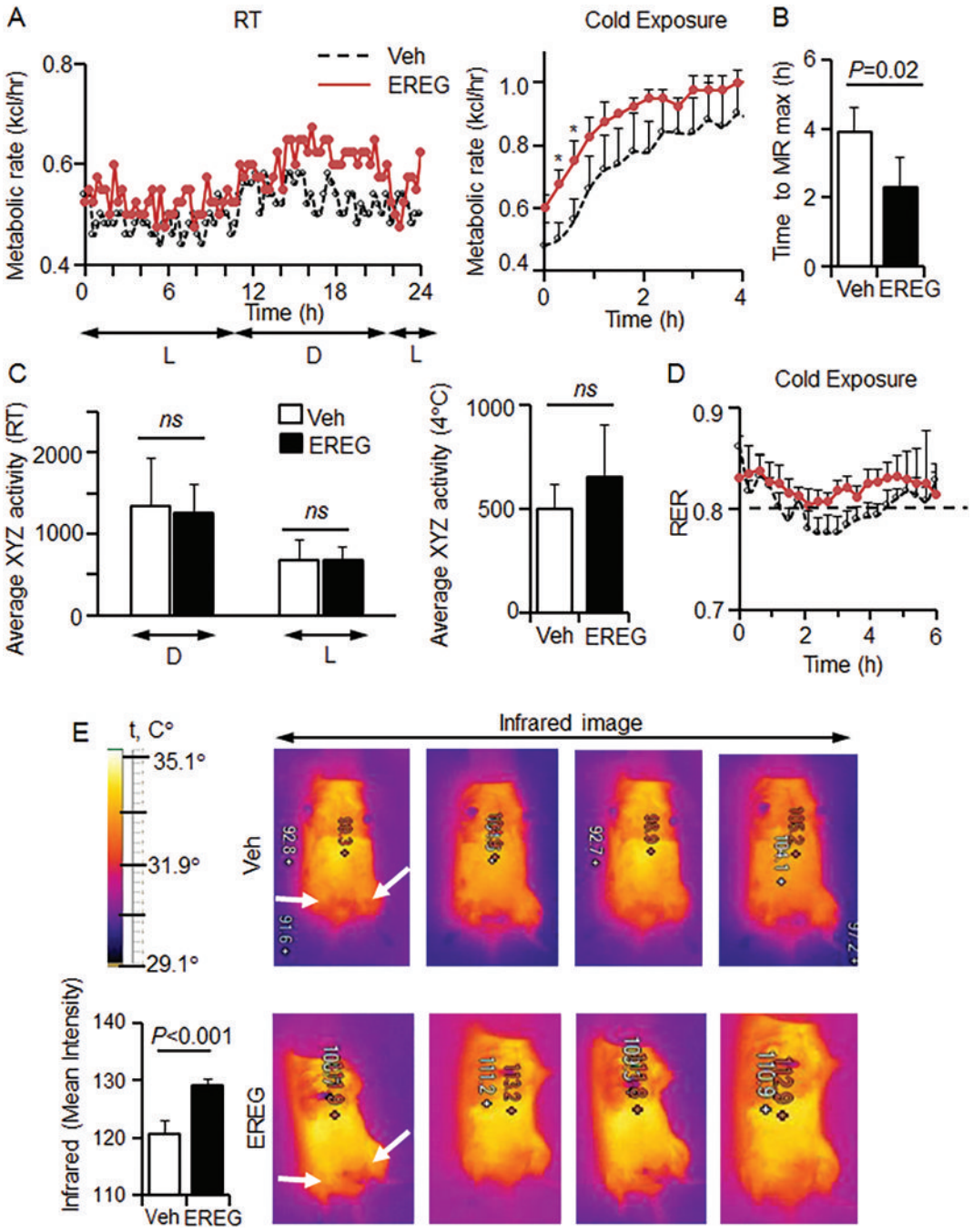

Figure 3.

EREG increases metabolic rate and core temperature in DIO mice. (A-D) DIO mice (n=4/group) were placed in individual metabolic cages equipped with CLAMS. Number of mice was limited by capacity of facility. Mice were randomly selected from whole group (A) Metabolic rate in PBS-(open circles) and EREG-injected (closed red circles) mice were analyzed at room temperature (RT, left panel) and during cold exposure (4°C, right panel). Data represent mean±SEM. (B) Metabolic rate (MR) kinetics during cold exposure was used to measure time until control (white bar) and EREG-treated mice (black bar) reached MR

maximum. Independent Student's *t*-test (C) locomotor XYZ activity at room temperature (RT, left panel) and during cold exposure (4°C, right panel). (mean±SD), Independent Student's *t*-test. (D) RER during cold exposure (mean±SD). (E) Body temperature scans (thermomap) DIO mice groups measured after cold exposure (mean±SD, n=4/group). Arrow indicates the injected sites after cold exposure. Yellow color indicates increased temperature in DIO mice treated with EREG vs mice injected with PBS (Veh). Temperature was quantified within same size iAb areas (Numbers inside animals were generated by camera's software to indicate highest and lowest point of measurements that are irrelevant to iAb temperature). Student's *t*-test.

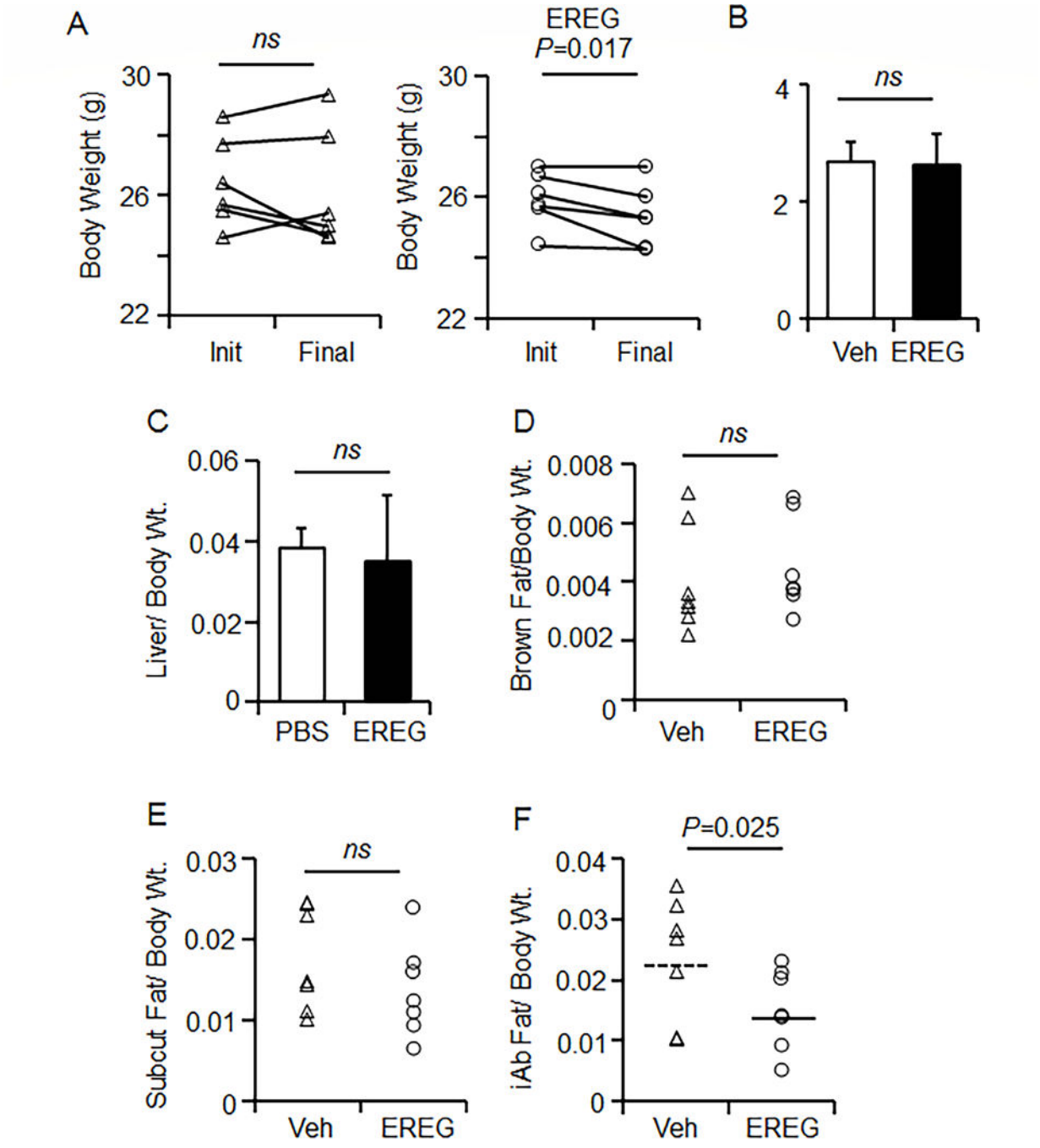

Figure 4.

EREG reduces iAb obesity in DIO mice. (A) Initial and final body weight comparison in Veh- and EREG treated DIO mice. The changes in body weights within groups (n=7/group, paired Student's *t*-test). Triangles and circles show weight of individual mice in the control and EREG-treated groups, respectively. (B) Food intake in the pair fed Veh- and EREG treated DIO mice. Mann-Whitney U test. (C-F) Weight of liver (C), brown fat (D), subcutaneous fat (E), and iAb fat (F). Organ weight was normalized to body weight. Data are shown as individual values, means are indicated as dashed (Veh) and solid (EREG-

treated) lines. Within-Subjects ANOVA, with sphericity a=0.25 and non-parametric one-sample run test.

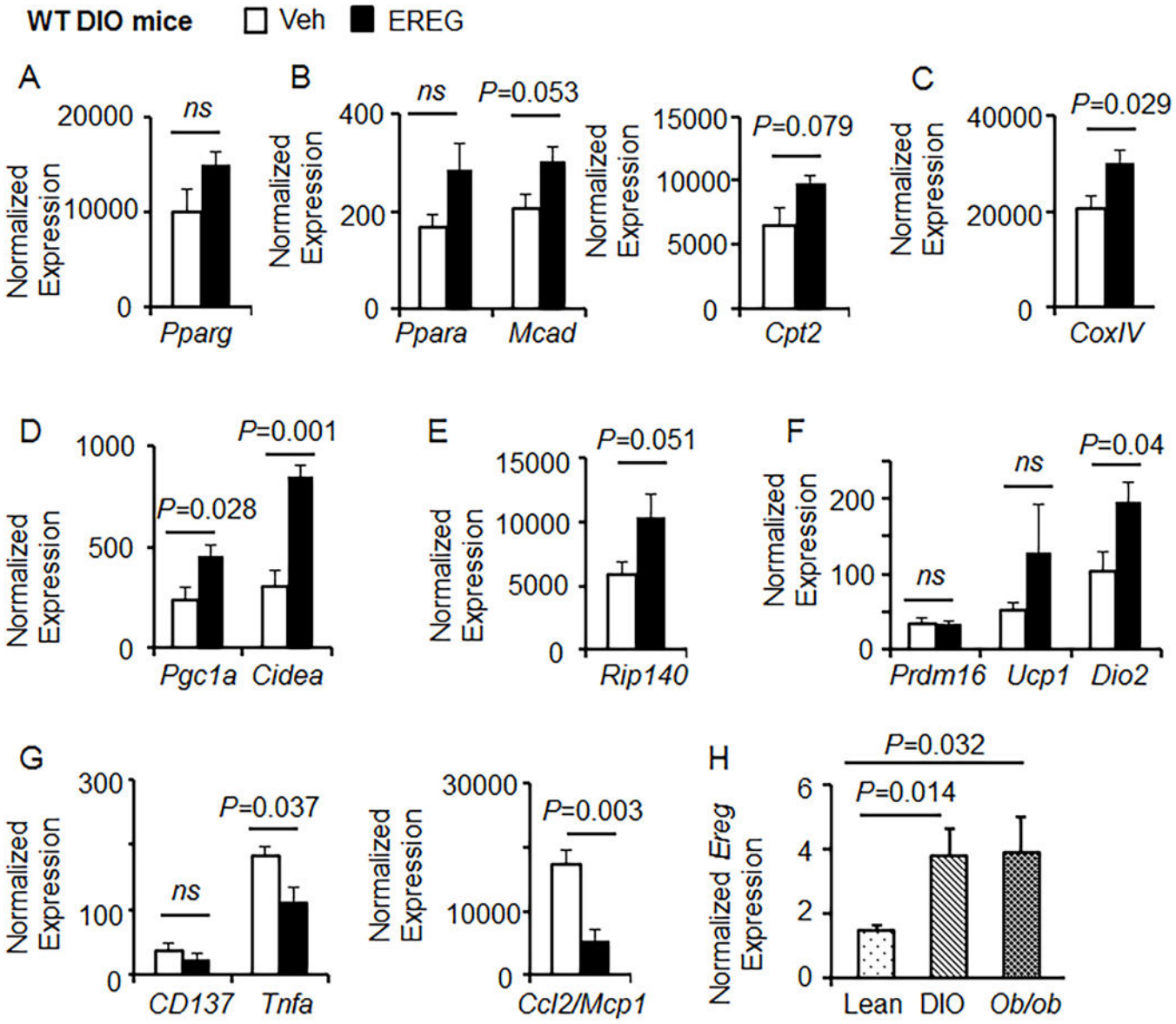

Figure 5.

EREG upregulates expression of thermogenic and PPARα-target genes, and downregulates inflammatory genes. (A-G) Gene expression was measured in total mRNA isolated from whole iAb fat pads of Veh- (white bars) and EREG-treated (black bars) DIO mice using NanoString assay. Gene expression was normalized to the expression of three housekeeping genes. Expression of markers for adipogenesis: (A) *Pparg*; mitochondrial fatty acid oxidation: (B) *Ppara*, *Mcad*, *Cpt2*; oxidative phosphorylation: (C) *CoxIV*; thermogenesis: (D) *Pgc1a*, *Cidea*, (E) *Rip140*, (F) *Prdm16*, *Ucp1*, *Dio2*; and inflammatory gene expression: (G) *CD137*, *Tnfa*, *Ccl2/Mcp1* were analyzed. Data represent mean±SD, n=5; Mann-Whitney U test (*Ucp1*) and independent Student's *t*-test (except *Ucp1*). (H) Similar *Ereg* expression analysis was performed in mRNA isolated from whole iAb fat pads of lean, DIO, and *ob/ob* mice (n=8/group) using NanoString assay. Data show mean±SD, Independent Student's *t*-test.

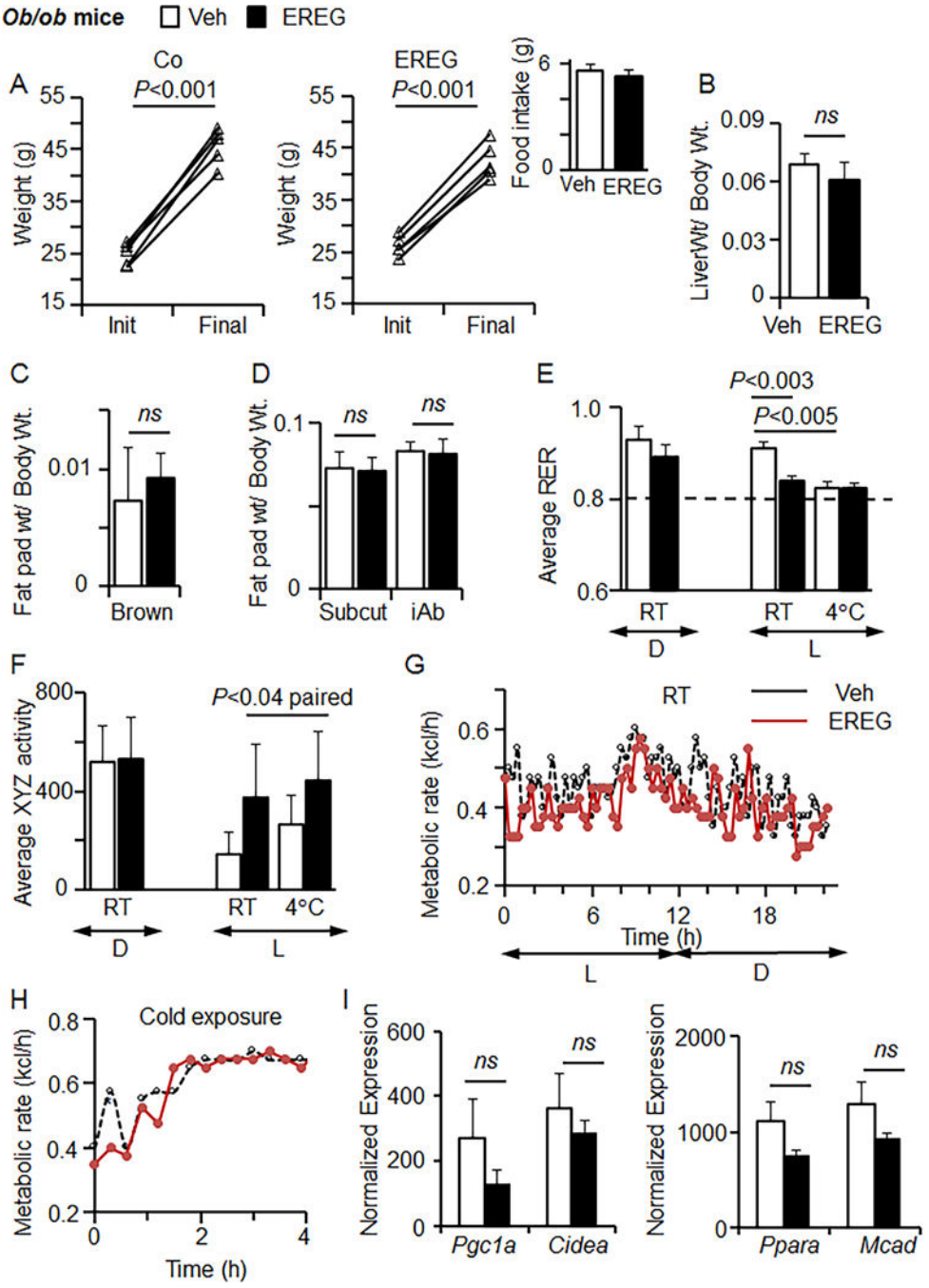

Figure 6.

Leptin deficiency abolishes EREG-mediated energy expenditure. (A) Body weight in *ob/ob* mice (n=5/group) before and after treatment with PBS (Veh) (open circles) or EREG (closed circles, 2.7 ng/g body weight). Insert shows food intake in these *ob/ob* mouse groups, which were pair-fed a high-fat diet throughout this study. (B) Liver, (C) BAT, (D) subcutaneous and iAb fat pad weight. Organ weight was normalized to body weight. (E-H) Metabolic parameters were analyzed in the same Veh and EREG-injected *ob/ob* mice (n=4/group) at RT and after cold exposure in metabolic cages equipped with CLAMS. (E) RER (mean

±SD), (F) locomotor activity (mean±SD), and (G,H) metabolic rate kinetics were measured in Veh-treated (white bars, or open circles) and EREG-treated (black bars, or closed circles) *ob/ob* mice. D and L represent 'dark' and 'light' cycles. (I) Expression of thermogenic (*Pgc1a*, *Cidea*) and PPARα, and its target gene *Mcad* in iAb fat from *ob/ob* mice was analyzed using NanoString mouse metabolic panel. Data show mean±SD, Independent Student's *t*-test (*Cidea*) and Mann-Whitney U test (except *Cidea*).